

Article

# Unscented Kalman Filtering for Nonlinear Systems with Stochastic Nonlinearities under FlexRay Protocol

Xianzheng Meng<sup>1,2,3</sup>, Hanbo Wang<sup>1,2,3</sup>, Yongxin Li<sup>1,2,3</sup>, and Yuxuan Shen<sup>1,2,3,\*</sup><sup>1</sup> Artificial Intelligence Energy Research Institute, Northeast Petroleum University, Daqing 163318, China<sup>2</sup> Heilongjiang Provincial Key Laboratory of Networking and Intelligent Control, Northeast Petroleum University, Daqing 163318, China<sup>3</sup> National Key Laboratory of Continental Shale Oil of China, Northeast Petroleum University, Daqing 163318, China\* Correspondence: [shenyuxuan5973@163.com](mailto:shenyuxuan5973@163.com)

Received: 13 January 2025

Accepted: 4 May 2025

Published: 27 June 2025

**Abstract:** In this paper, an unscented Kalman filtering problem is considered for a class of nonlinear systems with stochastic nonlinearities under the FlexRay protocol. The phenomenon of stochastic nonlinearities is characterized by the statistical means to account for engineering practice. Moreover, with the FlexRay protocol implemented between the sensors and the filter, an appropriate measurement model is established to characterize the measurement outputs after data transmission via the FlexRay protocol. By considering the stochastic nonlinearities and the FlexRay protocol, an tailored unscented Kalman filtering algorithm is designed where the influence of the stochastic nonlinearities and the FlexRay protocol is quantified. In the end, the effectiveness of the proposed filtering algorithm is verified in estimating the state of nonlinear systems through simulation experiments.

**Keywords:** Unscented Kalman Filter; nonlinear systems; FlexRay protocols; stochastic nonlinearities

## 1. Introduction

In recent decades, the rapid development of communication technology has propelled the application of wireless communication networks. Nowadays, an increasing number of industrial control systems communicate and connect through wireless communication networks, which are known as the networked control systems (NCSs) [1]. Compared to the traditional systems, the NCSs have advantages in decreasing the construction costs and improving the reliability of the system. As a result, the NCSs have found extensive applications in numerous fields such as power system management, drone control, and transportation [2–5]. Despite the advantages provided by the NCSs, some new challenges have also been brought to the corresponding control and state estimation problems [6]. Constrained by the limited bandwidth and transmission capacity of the wireless communication network, data transmissions in NCSs are prone to various network-induced issues including packet dropouts, time delays, and data quantization. Recently, plenty of researchers have conducted promising research to deal with these network-induced challenges and fruitful results have been obtained [7–9].

The filtering problem has long been a research hotspot in real engineering and has found extensive applications in areas such as environmental monitoring and target tracking [10–12]. The filtering technology offers an efficient method to extract valuable state information from measurements with noises, thereby ensuring the precision and dependability of system operation [13]. Notably, conventional linear filtering techniques are often unable to meet the practical requirements since the nonlinearities are ubiquitous in real-world systems [14, 15]. As such, the investigation on nonlinear filtering technologies is of paramount importance. To address this problem, plenty of nonlinear filtering techniques have been developed [16]. For instance, the extended Kalman filter estimates the system state by first linearizing the nonlinearities and then applying standard Kalman filtering procedures [17, 18]. Unfortunately, the extended Kalman filter does have its limitations, e.g. when dealing with highly nonlinear systems, the linearization error can largely undermine the filtering accuracy.

To achieve satisfactory filtering performance for nonlinear systems with severely nonlinearities, the unscented



Kalman filtering (UKF) approach has been developed [19, 20]. With the unscented Kalman filter, the linearization of nonlinearity is no longer needed and the calculation of the Jacobian matrix is spared. Instead, the unscented transformation is employed to approximate the probability density function which shows superiority in handling high-order nonlinearities [21–23]. Due to this advantage, the unscented Kalman filter has been widely studied and applied to various systems. For example, the UKF problem has been considered in [24] for complex networks with quantizations and amplify-and-forward relays. In [25], the unscented Kalman filter has been designed for unmanned aerial vehicles under the dynamic event-triggered protocol.

As mentioned before, the limited bandwidth of the wireless communication network inevitably leads to data collisions and brings undesired network-induced phenomena [26–28]. To address this issue, researchers have developed various kinds of communication protocols whose aim is to eliminate/reduce the data collisions by orchestrating the data transmissions based on certain principles [29, 30]. To date, the communication protocols that have been widely investigated in the signal processing area include the Round-Robin protocol (RRP) [31], the weighted Try-Once-Discard protocol (WTODP) [32], the stochastic communication protocol [33], and the FlexRay protocol [34, 35]. Among others, the FlexRay protocol incorporates both time-triggered and event-triggered selection principles, which not only ensures real-time transmission of time-sensitive information, but also dynamically adjusts the transmission priority according to the importance of the information. Therefore, the FlexRay protocol is able to ensure the transmission of critical information and improve the stability and efficiency of the system. Due to its advantages, the FlexRay protocol has been used in a variety of applications such as robot control systems, drone control systems and navigation systems [36, 37]. To date, scholars have investigated state estimation problems under the FlexRay protocol and have obtained considerable research results [38–40]. Nevertheless, it has been found that the UKF problems under the FlexRay protocol have received inadequate attention which motivates the current research.

Based on the above discussion, in this paper, we aim to study the UKF problem for nonlinear systems with stochastic nonlinearities under the FlexRay protocols. The challenges will be encountered are: 1) how to precisely describe the scheduling effect of the FlexRay protocol and integrate it in the framework of unscented Kalman filter? and 2) how to characterize the impact of the FlexRay protocol and stochastic nonlinearities on the filtering performance? By solving these challenges, the main contributions of this paper are reflected in the following aspects: 1) a mathematical model is proposed to describe the measurement under the FlexRay protocol which is then used to design the unscented Kalman filter; 2) both the impact of the FlexRay protocol and the stochastic nonlinearities are reflected in the developed filtering algorithm; and 3) the desired filter is explicitly presented based on the developed UKF algorithm.

The structure of the remaining sections of this paper is as follows. In Section II, the underlying nonlinear system with stochastic nonlinearities is constructed and the scheduling rule of the FlexRay protocol is described. Moreover, the measurement model under the FlexRay protocol is developed. In Section III, the UKF algorithm is designed and a simulation example is given in Section IV to verify the effectiveness of the developed filtering algorithm. Finally, the conclusion is presented in Section V.

**Notation.** The notations used in this paper are standard.  $A^T$  and  $A^{-1}$  are the transpose and inverse of matrix  $A$ , respectively.  $\text{diag}\{\dots\}$  denotes a diagonal matrix.  $\text{col}\{\dots\}$  denotes a column vector.  $\mathbb{E}\{x\}$  means the expectation of random variable  $x$  and  $\mathbb{E}\{x|y\}$  describes the expectation of  $x$  conditional on  $y$ .  $\delta(i, j)$  is the Kronecker delta function.  $\text{mod}(a, b)$  is the nonnegative remainder of  $a/b$ .

## 2. Problem formulations

In this paper, we consider the following discrete time-varying nonlinear system:

$$\begin{cases} x_{s+1} = f(x_s) + g(x_s, \eta_s) + w_s \\ y_s = h(x_s) + b(x_s, \zeta_s) + v_s \end{cases} \quad (1)$$

where  $x_s \in \mathbb{R}^n$  is the state of the system,  $y_s \in \mathbb{R}^m$  is the measurement output,  $w_s \in \mathbb{R}^n$  is the zero-mean process noise with covariance  $Q_s > 0$ , and  $v_s \in \mathbb{R}^m$  is the zero-mean measurement noise with covariance  $R_s > 0$ .  $f(\cdot) : \mathbb{R}^n \rightarrow \mathbb{R}^n$  and  $h(\cdot) : \mathbb{R}^n \rightarrow \mathbb{R}^m$  are known nonlinear functions.  $\eta_s$  and  $\zeta_s$  are zero-mean Gaussian disturbances. It is assumed that  $\eta_s, \zeta_s, w_s, v_s$  are uncorrelated with each other. Moreover, the measurement outputs are transmitted in  $N$  ( $N \leq m$ ) data packets from  $N$  transmission nodes, i.e.  $y_s = [y_{1,s} \ \dots \ y_{N,s}]^T \in \mathbb{R}^m$  where  $y_{i,s} \in \mathbb{R}^{m_i}$  with  $\sum_{i=1}^N m_i = m$ .

The stochastic nonlinearities  $g(x_s, \eta_s) : \mathbb{R}^n \times \mathbb{R}^n \rightarrow \mathbb{R}^n$  and  $b(x_s, \zeta_s) : \mathbb{R}^n \times \mathbb{R}^n \rightarrow \mathbb{R}^m$  satisfy  $g(0, \eta_s) = b(0, \zeta_s) = 0$  and

$$\begin{aligned} \mathbb{E} \left\{ \begin{bmatrix} g(x_s, \eta_s) \\ b(x_s, \zeta_s) \end{bmatrix} \middle| x_s \right\} &= 0, \\ \mathbb{E} \left\{ \begin{bmatrix} g(x_s, \eta_s) \\ b(x_s, \zeta_s) \end{bmatrix} \begin{bmatrix} g(x_j, \eta_j) \\ b(x_j, \zeta_j) \end{bmatrix}^T \middle| x_s \right\} &= 0, s \neq j, \\ \mathbb{E} \{ g(x_s, \eta_s) g^T(x_s, \eta_s) | x_s \} &= \Pi_s^1 x_s^T \Gamma_s^1 x_s, \\ \mathbb{E} \{ b(x_s, \zeta_s) b^T(x_s, \zeta_s) | x_s \} &= \Pi_s^2 x_s^T \Gamma_s^2 x_s \end{aligned}$$

where  $\Pi_s^1, \Pi_s^2, \Gamma_s^1$  and  $\Gamma_s^2$  are known matrices.

In practice, the limitation of network bandwidth often makes the network-induced phenomena inevitable [41, 42]. To address this challenge, different kinds of communication protocols have been designed to optimize data transmissions so as to save the limited bandwidth. In this paper, the FlexRay protocol is employed to orchestrate the sensor nodes.

As shown in Figure 1, a communication cycle of the FlexRay protocol usually contains a static segment, a dynamic segment, a symbol window and a network idle time [43]. The time lengths of the static segment and dynamic segment are defined as  $R_1 = l$  ( $l < N$ ) and  $R_2 = 1$ , respectively. Since the time lengths of the symbol window and the network idle time are usually very short, so their time lengths are defined as  $R_3 = R_4 = 0$ . Therefore, it can be concluded that the time length of one communication cycle is  $l_1 \triangleq l + 1$ . During the static segment, the RRP is used to regulate the transmission of  $y_{\epsilon,s}$  ( $\epsilon \in \{1, 2, \dots, l\}$ ). During the dynamic segment, the WTODP is used to regulate the transmission of  $y_{\epsilon,s}$  ( $\epsilon \in \{l + 1, l + 2, \dots, N\}$ ).

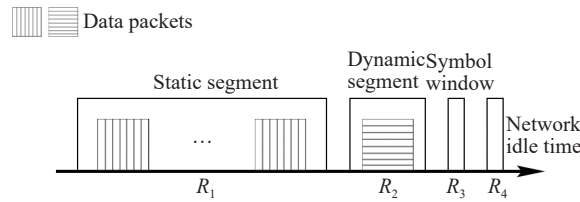


**Figure 1.** A communication cycle under the FlexRay protocol.

Now, let's discuss how the FlexRay protocol affects the sensor-to-filter transmission. First, we denote

$$\begin{aligned} y_s &\triangleq \text{col}\{y_s^1, y_s^2\}, \\ \bar{y}_s &\triangleq \text{col}\{\bar{y}_s^1, \bar{y}_s^2\}, \\ y_s^1 &\triangleq \text{col}\{y_{1,s}, \dots, y_{l,s}\}, \\ y_s^2 &\triangleq \text{col}\{y_{l+1,s}, \dots, y_{N,s}\}, \\ \bar{y}_s^1 &\triangleq \text{col}\{\bar{y}_{1,s}, \dots, \bar{y}_{l,s}\}, \\ \bar{y}_s^2 &\triangleq \text{col}\{\bar{y}_{l+1,s}, \dots, \bar{y}_{N,s}\}. \end{aligned}$$

From the principle of the FlexRay protocol, we know that  $y_s^1$  is scheduled by the RRP and  $y_s^2$  is scheduled by the WTODP.  $\bar{y}_s^1$  and  $\bar{y}_s^2$  denote the received measurement outputs by the filter after transmission over the network under the RRP and the WTODP, respectively.

In what follows, we will characterize  $\bar{y}_s^1$  and  $\bar{y}_s^2$  by resorting to the principle of the RRP and the WTODP. Denote  $\vartheta_s$  and  $\tau_s$  as the sensor node that is allowed to transmit at time instant  $s$  under the RRP and the WTODP, respectively. According to the scheduling rule of the RRP, we know that

$$\vartheta_s = \begin{cases} \text{mod}(s - q, l) + 1, & s \in \mathbb{R}_1, \\ 0, & s \in \mathbb{R}_2 \end{cases} \quad (2)$$

where  $\mathbb{R}_1 \triangleq \{(q - 1)l_1 + 1, (q - 1)l_1 + l\}$  and  $\mathbb{R}_2 \triangleq ql_1$  ( $q = 1, 2, 3, \dots$ ). Moreover, the zero-order holder strategy is used on the filter to generate the measurement of the sensors that didn't get the transmission access [44]. According to (2) and the zero-order holder strategy, the actual measurement output at the filter side can be written as

$$\bar{y}_{\epsilon,s} = \begin{cases} y_{\epsilon,s}, & \epsilon = \vartheta_s, \\ \bar{y}_{\epsilon,s-1}, & \epsilon \neq \vartheta_s \end{cases} \quad (3)$$

for  $\epsilon \in \{1, 2, \dots, l\}$ .

Similarly, based on the scheduling rule of the WTODP, the selected node can be decided by

$$\tau_s = \begin{cases} \operatorname{argmax}_{j \in \{l+1, l+2, \dots, N\}} \tilde{y}_{j,s}^T Q_{j,s} \tilde{y}_{j,s}, & s \in \mathbb{R}_2, \\ 0, & s \in \mathbb{R}_1 \end{cases} \quad (4)$$

where  $\tilde{y}_{j,s} \triangleq y_{j,s} - \bar{y}_{j,s-1}$  and  $Q_{j,s} > 0$  is a known matrix. Based on (4) and the zero-order holder strategy, the actual measurement output at the filter side is

$$\bar{y}_{\epsilon,s} = \begin{cases} y_{\epsilon,s}, & \epsilon = \tau_s, \\ \bar{y}_{\epsilon,s-1}, & \epsilon \neq \tau_s \end{cases} \quad (5)$$

for  $\epsilon \in \{l+1, l+2, \dots, N\}$ .

Define  $\Phi_{\theta_s} \triangleq \operatorname{diag}\{\delta(1, \theta_s), \delta(2, \theta_s), \dots, \delta(l, \theta_s)\}$  and  $\Phi_{\tau_s} \triangleq \operatorname{diag}\{\delta(l+1, \tau_s), \dots, \delta(N, \tau_s)\}$ . Based on (3) and (5),  $\bar{y}_s^1$  and  $\bar{y}_s^2$  are rewritten as

$$\bar{y}_s^1 = \begin{cases} \Phi_{\theta_s} y_s^1 + (I - \Phi_{\theta_s}) \bar{y}_{s-1}^1, & s \in \mathbb{R}_1, \\ \bar{y}_{s-1}^1, & s \in \mathbb{R}_2, \end{cases} \quad (6)$$

$$\bar{y}_s^2 = \begin{cases} \bar{y}_{s-1}^2, & s \in \mathbb{R}_1, \\ \Phi_{\tau_s} y_s^2 + (I - \Phi_{\tau_s}) \bar{y}_{s-1}^2, & s \in \mathbb{R}_2. \end{cases} \quad (7)$$

From the discussion on the FlexRay protocol, it is obvious that there exists a switching between the RRP and the WTODP in each communication cycle. By introducing

$$p_s \triangleq \begin{cases} 0, & s \in \mathbb{R}_1, \\ 1, & s \in \mathbb{R}_2, \end{cases} \quad (8)$$

the actual measurement  $\bar{y}_s$  at the filter side is

$$\begin{aligned} \bar{y}_s &= (1-p_s)(\bar{I}_1 \Phi_{\theta_s} y_s^1 + \bar{I}_1 (I - \Phi_{\theta_s}) \bar{y}_{s-1}^1 + \bar{I}_2 \bar{y}_{s-1}^2) \\ &\quad + p_s(\bar{I}_1 \bar{y}_{s-1}^1 + \bar{I}_2 \Phi_{\tau_s} y_s^2 + \bar{I}_2 (I - \Phi_{\tau_s}) \bar{y}_{s-1}^2) \\ &= ((1-p_s) \bar{I}_1 \Phi_{\theta_s} \bar{I}_1^T + p_s \bar{I}_2 \Phi_{\tau_s} \bar{I}_2^T) y_s \\ &\quad + ((1-p_s) \Theta_s^1 + p_s \Theta_s^2) \bar{y}_{s-1} \end{aligned} \quad (9)$$

where

$$\begin{aligned} \Theta_s^1 &\triangleq \begin{bmatrix} \bar{I}_1 (I - \Phi_{\theta_s}) & \bar{I}_2 \end{bmatrix}, \\ \Theta_s^2 &\triangleq \begin{bmatrix} \bar{I}_1 & \bar{I}_2 (I - \Phi_{\tau_s}) \end{bmatrix}, \\ \bar{I}_1 &\triangleq \begin{bmatrix} I_l \\ 0_{(N-l) \times l} \end{bmatrix}, \quad \bar{I}_2 \triangleq \begin{bmatrix} 0_{l \times (N-l)} \\ I_{N-l} \end{bmatrix}. \end{aligned}$$

For convenience of later analysis, we denote  $\hat{x}_{s+1|s}$  and  $\hat{x}_{s+1|s+1}$  as the one-step prediction and the estimate of the state at time instant  $s+1$ , respectively. Moreover, we set the one-step prediction error and the filtering error be  $\tilde{x}_{s+1|s} \triangleq x_{s+1} - \hat{x}_{s+1|s}$  and  $\tilde{x}_{s+1|s+1} \triangleq x_{s+1} - \hat{x}_{s+1|s+1}$ , respectively. Accordingly, the one-step prediction error covariance is  $\hat{P}_{s+1|s} \triangleq \mathbb{E}\{\tilde{x}_{s+1|s} \tilde{x}_{s+1|s}^T\}$  and the filtering error covariance is  $\hat{P}_{s+1|s+1} \triangleq \mathbb{E}\{\tilde{x}_{s+1|s+1} \tilde{x}_{s+1|s+1}^T\}$ . In this paper, we aim to design an unscented Kalman filtering algorithm for nonlinear systems under the FlexRay protocol which is able to effectively deal with the effect of stochastic nonlinearities.

### 3. Main results

The design of an UKF algorithm under the FlexRay protocol is investigated in this section.

#### 3.1. Unscented transform

The unscented transform for discrete-time nonlinear systems can be summarised as follows. Choose a sigma point set  $\chi_s = \{\chi_{0,s}, \dots, \chi_{2n,s}\}$  which contains  $2n+1$  sigma points. The sigma points with known mean  $\hat{x}_{s|s}$  and covariance  $\hat{P}_{s|s}$  are selected by

$$\begin{aligned} \chi_{0,s} &= \hat{x}_{s|s}, \\ \chi_{j,s} &= \hat{x}_{s|s} + \iota_{j,s}, \quad j = 1, 2, \dots, n \\ \chi_{j,s} &= \hat{x}_{s|s} - \iota_{j,s}, \quad j = n+1, n+2, \dots, 2n \end{aligned} \quad (10)$$

where  $\iota_{j,s} = (\sqrt{(n+\gamma)\hat{P}_{s|s}})_j$  denotes the  $j$ th column of  $\sqrt{(n+\gamma)\hat{P}_{s|s}}$  and  $\gamma = n(\alpha^2 - 1)$  is a proportion parameter with  $0 \leq \alpha \leq 1$ .

To obtain  $\hat{x}_{s+1|s}$  and  $\hat{P}_{s+1|s}$ , two weighted coefficients  $\theta_j^m$  and  $\theta_j^c$  are chosen as

$$\begin{aligned} \theta_0^m &= \frac{\gamma}{n + \gamma}, \\ \theta_0^c &= \frac{\gamma}{n + \gamma} + (1 - \alpha^2 + \beta), \\ \theta_j^m &= \theta_j^c = \frac{1}{2(n + \gamma)}, \quad j = 1, 2, \dots, 2n \end{aligned}$$

where  $\beta > 0$  is chosen based on the prior knowledge of the system state.

**Remark 1** It can be seen that the selection of sigma points affects the computational complexity of the unscented Kalman filtering algorithm. The number of sigma points is usually set to be  $2n + 1$  where  $n$  is the dimension of the system state. The computational complexity rises significantly while increasing  $n$ .  $\gamma$  and  $\alpha$  are important parameters used to adjust the distribution of sigma points and weighting coefficients. Their selection not only affects the accuracy and stability of the algorithm but also has a certain impact on the computational complexity. Smaller  $\gamma$  and  $\alpha$  will reduce the distance between the sigma points and the mean value, thus reducing the scale of the matrix operation and leading to a decrease in computational complexity.

Propagating the  $2n + 1$  sigma points through the nonlinear function  $f(\cdot)$  to obtain the following transformed sigma points  $\hat{\chi}_{j,s+1|s}$

$$\hat{\chi}_{j,s+1|s} = f(\chi_{j,s}) \quad j = 0, \dots, 2n. \tag{11}$$

Then, the one-step prediction  $\hat{x}_{s+1|s}$  of state can be obtained by

$$\hat{x}_{s+1|s} = \sum_{j=0}^{2n} \theta_j^m \hat{\chi}_{j,s+1|s} \tag{12}$$

and the one-step prediction error covariance  $\hat{P}_{s+1|s}$  is calculated by

$$\begin{aligned} \hat{P}_{s+1|s} &= \sum_{j=0}^{2n} \theta_j^c (\hat{\chi}_{j,s+1|s} - \hat{x}_{s+1|s})(\hat{\chi}_{j,s+1|s} - \hat{x}_{s+1|s})^T \\ &\quad + \mathbb{E}\{g(x_s, \eta_s)g^T(x_s, \eta_s)\} + Q_s \end{aligned} \tag{13}$$

where  $\mathbb{E}\{g(x_s, \eta_s)g^T(x_s, \eta_s)\}$  represents the covariance of the stochastic nonlinearities.

From (13), we know that the covariance of the sigma points  $\hat{\chi}_{j,s+1|s}$  is different with the covariance  $\hat{P}_{s+1|s}$  due to the stochastic nonlinearities and the noise. Therefore, to accurately predict the measurement output, we select another set of sigma points  $\{\varphi_{0,s+1}, \varphi_{1,s+1}, \dots, \varphi_{2n,s+1}\}$  with

$$\begin{aligned} \varphi_{0,s+1} &= \hat{x}_{s+1|s}, \\ \varphi_{j,s+1} &= \hat{x}_{s+1|s} + \psi_{j,s+1|s}, \quad j = 1, 2, \dots, n \\ \varphi_{j,s+1} &= \hat{x}_{s+1|s} - \psi_{j,s+1|s}, \quad j = n + 1, \dots, 2n \end{aligned} \tag{14}$$

where  $\psi_{j,s+1|s} = (\sqrt{(n + \gamma)\hat{P}_{s+1|s}})_j$  denotes the  $j$ th column of  $\sqrt{(n + \gamma)\hat{P}_{s+1|s}}$ .

Similarly, propagating the  $2n + 1$  sigma points through the nonlinear function  $h(\cdot)$  to obtain the following transformed sigma points  $\hat{\varphi}_{j,s+1|s}$

$$\hat{\varphi}_{j,s+1|s} = h(\varphi_{j,s+1}), \quad j = 0, \dots, 2n. \tag{15}$$

Then, the prediction  $\hat{y}_{s+1|s}$  of the measurement output is obtained by

$$\hat{y}_{s+1|s} = \sum_{j=0}^{2n} \theta_j^m \hat{\varphi}_{j,s+1|s}. \tag{16}$$

After obtaining the state prediction, the error covariance and the measurement output, in the next subsection, we will present the UKF algorithm in detail.

### 3.2. UKF Algorithm under the FlexRay protocol

In the following, we will obtain the UKF algorithm under the FlexRay protocol. First, under the FlexRay protocol, (15) and (16) are reformulated as

$$\begin{aligned} \hat{\varphi}_{j,s+1|s}^f &= (1 - p_{s+1})\bar{I}_1\Phi_{\theta_{s+1}}\bar{I}_1^T\hat{\varphi}_{j,s+1|s} \\ &\quad + p_{s+1}\bar{I}_2\Phi_{\tau_{s+1}}\bar{I}_2^T\hat{\varphi}_{j,s+1|s} \\ &\quad + (1 - p_{s+1})\Theta_{s+1}^1\hat{\varphi}_{j,s|s-1} \\ &\quad + p_{s+1}\Theta_{s+1}^2\hat{\varphi}_{j,s|s-1}, \end{aligned} \tag{17}$$

$$\begin{aligned} \hat{y}_{s+1|s}^f &= (1 - p_{s+1})\bar{I}_1\Phi_{\theta_{s+1}}\bar{I}_1^T\hat{y}_{s+1|s} \\ &\quad + p_{s+1}\bar{I}_2\Phi_{\tau_{s+1}}\bar{I}_2^T\hat{y}_{s+1|s} \\ &\quad + (1 - p_{s+1})\Theta_{s+1}^1\hat{y}_{s|s-1} \\ &\quad + p_{s+1}\Theta_{s+1}^2\hat{y}_{s|s-1} \end{aligned} \tag{18}$$

where  $\hat{\varphi}_{j,s+1|s}^f$  and  $\hat{y}_{s+1|s}^f$  denote the transformed sigma points and predicted measurement under the FlexRay protocol. Based on (17) and (18), the covariances  $\hat{P}_{yy,s+1|s}$  and  $\hat{P}_{xy,s+1|s}$  can be calculated by

$$\begin{aligned} \hat{P}_{yy,s+1|s} &= \sum_{j=0}^{2n} \theta_j^c (\hat{\varphi}_{j,s+1|s}^f - \hat{y}_{s+1|s}^f)(\hat{\varphi}_{j,s+1|s}^f - \hat{y}_{s+1|s}^f)^T \\ &\quad + \mathbf{N}_{s+1}(\mathbb{E}\{b(x_{s+1}, \zeta_{s+1})b^T(x_{s+1}, \zeta_{s+1})\} + R_{s+1})\mathbf{N}_{s+1}^T, \end{aligned} \tag{19}$$

$$\hat{P}_{xy,s+1|s} = \sum_{j=0}^{2n} \theta_j^c (\hat{\chi}_{j,s+1|s} - \hat{x}_{s+1|s})(\hat{\varphi}_{j,s+1|s}^f - \hat{y}_{s+1|s}^f)^T \tag{20}$$

where  $\mathbf{N}_{s+1} = (1 - p_{s+1})\bar{I}_1\Phi_{\theta_{s+1}}\bar{I}_1^T + p_{s+1}\bar{I}_2\Phi_{\tau_{s+1}}\bar{I}_2^T$  and  $\mathbb{E}\{b(x_{s+1}, \zeta_{s+1})b^T(x_{s+1}, \zeta_{s+1})\}$  represents the covariance of the stochastic nonlinearities. Then, we have the following unscented Kalman filter under the FlexRay protocol:

$$\hat{x}_{s+1|s+1} = \hat{x}_{s+1|s} + K_{s+1}(\bar{y}_{s+1} - \hat{y}_{s+1|s}^f), \tag{21}$$

$$\hat{P}_{s+1|s+1} = \hat{P}_{s+1|s} - K_{s+1}\hat{P}_{yy,s+1|s}K_{s+1}^T, \tag{22}$$

$$K_{s+1} = \hat{P}_{xy,s+1|s}(\hat{P}_{yy,s+1|s})^{-1}. \tag{23}$$

The UKF algorithm under the FlexRay protocol is summarized in Algorithm 1 based on the above analysis.

---

**Algorithm 1** The UKF algorithm under the FlexRay protocol

---

*Step 1.* Initialize the parameters  $\bar{x}_{0|0} = \hat{x}_{0|0}$ ,  $\bar{P}_{0|0} = \hat{P}_{0|0}$ . Select appropriate weighted coefficients  $\theta_0^m$ ,  $\theta_0^c$ ,  $\theta_j^m$  and  $\theta_j^c$  ( $j = 1, 2, \dots, 2n$ ). Let the time length of the communication cycle be  $l_1 = l + 1$ . Set  $s = 0$ ;

*Step 2.* At time instant  $s + 1$ , calculate  $2n + 1$  sigma points  $\chi_{j,s}$  with known  $\hat{x}_{s|s}$  and  $\hat{P}_{s|s}$ , then calculate one-step prediction state  $\hat{x}_{s+1|s}$  and one-step prediction error covariance  $\hat{P}_{s+1|s}$ ;

*Step 3.* Choose the node with transmission permission at the current time according to scheduling rules of the FlexRay protocol and calculate  $p_{s+1}$ ;

*Step 4.* Calculate  $2n + 1$  sigma points  $\varphi_{i,s+1}$ . Then, compute the prediction measurement  $\hat{y}_{s+1|s}^f$ , the covariance  $\hat{P}_{yy,s+1|s}$  and  $\hat{P}_{xy,s+1|s}$ .

Obtain the filter gain  $K_{s+1}$ , then update  $\hat{P}_{s+1|s+1}$  and  $\hat{x}_{s+1|s+1}$ ;

*Step 5.* If  $s + 1 < s_{max}$ , then let  $s = s + 1$  and go to Step 2, else go to Step 6;

*Step 6.* Stop.

---

#### 4. An illustrative example

In this section, an example is given to demonstrate the efficiency and applicability of the proposed UKF algorithm under the FlexRay protocol.

Consider a time-varying nonlinear system (1) with stochastic nonlinearities and the following parameters:

$$\begin{aligned} f(x_s) &= \begin{bmatrix} 0.58x_{1,s} + 0.3 \cos(s)x_{1,s} + 0.39x_{2,s} \\ 0.28x_{1,s} + 0.2 \sin(s)x_{1,s} + 0.52x_{2,s} \end{bmatrix} \\ h(x_s) &= \begin{bmatrix} 0.36x_{1,s} + x_{2,s}x_{2,s} \\ x_{1,s}x_{2,s} + 0.16x_{2,s} \\ 0.8 \cos(s)x_{1,s} + 0.36x_{2,s} \\ 0.5x_{1,s} + x_{1,s}x_{2,s} \\ 0.7 \cos(s)x_{1,s} + 0.8x_{2,s} \\ 0.3x_{1,s} + 0.8 \sin(s)x_{2,s} \end{bmatrix} \end{aligned}$$

where  $x_{i,s}$  ( $i = 1, 2$ ) is the  $i$ -th element of  $x_s$ . Furthermore, we set the covariance of the process noise as  $Q_s = 0.05I$  and the covariance of measurement noise as  $R_s = 0.01I$ , respectively. Supposed that  $N = 6$ , then  $y_s$  is denoted as  $y_s \triangleq \text{col} \{y_{1,s}, y_{2,s}, y_{3,s}, y_{4,s}, y_{5,s}, y_{6,s}\}$ .

In the simulation, we let the first four nodes be scheduled by the RRP and the last two nodes be scheduled by the WTODP. Therefore, the time length of the communication cycle of the FlexRay protocol is  $l_1 = l + 1 = 5$ .

The stochastic nonlinearities  $g(x_s, \eta_s)$  and  $b(x_s, \zeta_s)$  are given as

$$g(x_s, \eta_s) = \begin{bmatrix} 0.3 \\ 0.2 \end{bmatrix} [ 0.2x_{1,s}\eta_{1,s} + 0.3x_{2,s}\eta_{2,s} ]$$

$$b(x_s, \zeta_s) = U_1 \cdot [ 0.2x_{1,s}\zeta_{1,s} + 0.3x_{2,s}\zeta_{2,s} ]$$

where  $U_1 = [ 0.3 \ 0.2 \ 0.1 \ 0.1 \ 0.2 \ 0.3 ]^T$ .  $\eta_{i,s}$  and  $\zeta_{i,s}$  ( $i = 1, 2$ ) are the Gaussian white noises with zero-mean and unity covariance. From the stochastic nonlinearities, we know that

$$\mathbb{E}\{g(x_s, \eta_s)g^T(x_s, \eta_s)|x_s\} = \begin{bmatrix} 0.09 & 0.06 \\ 0.06 & 0.04 \end{bmatrix} x_s^T \begin{bmatrix} 0.04 & 0 \\ 0 & 0.09 \end{bmatrix} x_s,$$

$$\mathbb{E}\{b(x_s, \zeta_s)b^T(x_s, \zeta_s)|x_s\} = U_2 x_s^T \begin{bmatrix} 0.04 & 0 \\ 0 & 0.09 \end{bmatrix} x_s$$

where

$$U_2 = \begin{bmatrix} 0.09 & 0.06 & 0.03 & 0.03 & 0.06 & 0.09 \\ 0.06 & 0.04 & 0.02 & 0.02 & 0.04 & 0.06 \\ 0.03 & 0.02 & 0.01 & 0.01 & 0.02 & 0.03 \\ 0.03 & 0.02 & 0.01 & 0.01 & 0.02 & 0.03 \\ 0.06 & 0.04 & 0.02 & 0.02 & 0.04 & 0.06 \\ 0.09 & 0.06 & 0.03 & 0.03 & 0.06 & 0.09 \end{bmatrix}.$$

In the simulation, the initial values are set as  $\hat{x}_{0|0} = \bar{x}_{0|0} = [5 \ -2]^T$  and  $\hat{P}_{0|0} = \bar{P}_{0|0} = \text{diag}\{1, 1\}$ . For the unscented transform, the weighted coefficients are selected as  $\alpha = 1$ ,  $\beta = 2$ ,  $\gamma = 0$ . With the given parameters, we can calculate the filter gain and obtain the simulation results as shown in [Figures 2-5](#).

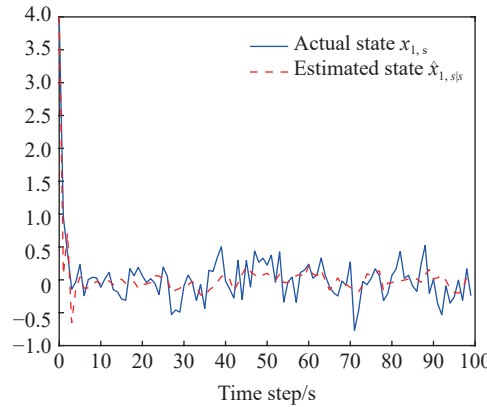


**Figure 2.** State  $x_{1,s}$  and its estimate  $\hat{x}_{1,s}$ .

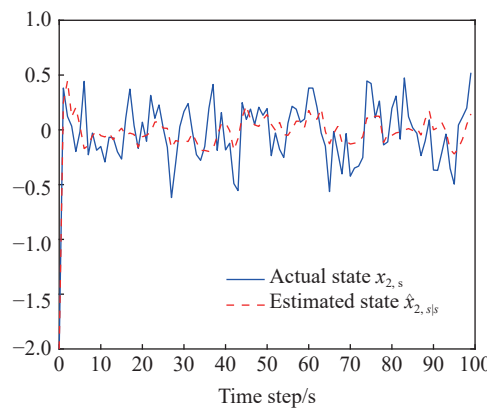


**Figure 3.** State  $x_{2,s}$  and its estimate  $\hat{x}_{2,s}$ .

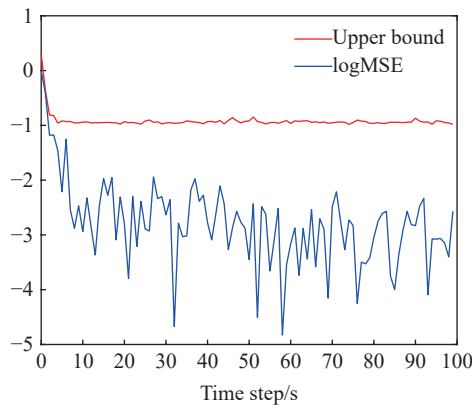


**Figure 4.**  $\{\log\text{MSE}\}$  and its upper bound.

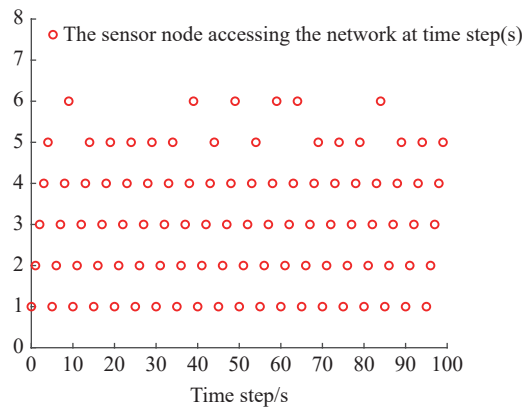


**Figure 5.** The sensor node accessing the network.

In the simulation results, [Figure 2](#) and [Figure 3](#) describe the trajectories of the actual states  $x_{i,s}$  and the estimates  $\hat{x}_{i,s|s}$ , respectively. The mean square error (MSE) is calculated by  $\text{MSE} = \frac{1}{i} \sum_{s=1}^S (x_{1,s} - \hat{x}_{1,s|s})^2 + (x_{2,s} - \hat{x}_{2,s|s})^2$  with  $S = 100$ . As can be observed from [Figure 4](#), the log of MSE is consistently maintained below the log of the upper bound. From [Figures 2-4](#), it is evident that the proposed UKF algorithm shows satisfactory performance.

The effect of the FlexRay protocol on the measurement outputs is shown in [Figure 5](#) with the sensor nodes being granted the transmission access at time instant  $s$ . From [Figure 5](#), we can see that the data transmission is effectively reduced. In conclusion, the algorithm proposed in this paper shows significant effectiveness in dealing state estimation problems with stochastic nonlinearities under the FlexRay protocol.

## 5. Conclusion

In this paper, an UKF algorithm has been designed for nonlinear systems with stochastic nonlinearities under the FlexRay protocol. First, a novel measurement model that characterizes the scheduling effect of the FlexRay protocol has been established. Then, a novel unscented transformation has been conducted by taking into account the FlexRay protocol and the stochastic nonlinearities. With the novel unscented transformation, the unscented Kalman filtering algorithm has been designed where the influence from the FlexRay protocol and the stochastic nonlinearities has been quantified. Finally, a simulation experiment has been provided whose results show that the proposed algorithm is effective in estimating the state of nonlinear systems under the FlexRay protocol. In the future, we could further explore applications of the proposed algorithm in intelligent manufacture [\[45\]](#) and sensor networks [\[46\]](#). For example, in intelligent manufacture, the algorithm can be used for predictive maintenance and cost control. In sensor networks, the algorithm can be used for distributed state estimation. These potential applications provide new directions for the development of the unscented Kalman filtering algorithm.

**Author Contributions:** **Xianzheng Meng:** Conceptualization, Methodology, Software, Writing-original draft; **Hanbo Wang:** Methodology, Software, Writing-review & editing; **Yongxin Li:** Software, Writing-original draft; **Yuxuan Shen:** Supervision, Conceptualization, Methodology, Writing-review & editing.

**Funding:** This work was supported by the Hainan Province Science and Technology Special Fund under Grant ZDYF2022SHFZ105.

**Data Availability Statement:** Not applicable.

**Conflicts of Interest:** The authors declare no conflict of interest.

## References

1. Pan, Y.N.; Wu, Y.M.; Lam, H.K. Security-based fuzzy control for nonlinear networked control systems with DoS attacks via a resilient event-triggered scheme. *IEEE Trans. Fuzzy Syst.*, **2022**, *30*, 4359–4368. doi: [10.1109/TFUZZ.2022.3148875](https://doi.org/10.1109/TFUZZ.2022.3148875)
2. Li, X.G.; Feng, S.; Hou, N.; *et al.* Surface microseismic data denoising based on sparse autoencoder and Kalman filter. *Syst. Sci. Control Eng.*, **2022**, *10*, 616–628. doi: [10.1080/21642583.2022.2087786](https://doi.org/10.1080/21642583.2022.2087786)
3. Pang, Z.H.; Fan, L.Z.; Sun, J.; *et al.* Detection of stealthy false data injection attacks against networked control systems via active data modification. *Inf. Sci.*, **2021**, *546*, 192–205. doi: [10.1016/j.ins.2020.06.074](https://doi.org/10.1016/j.ins.2020.06.074)
4. Hu, J.; Jia, C.Q.; Yu, H.; *et al.* Dynamic event-triggered state estimation for nonlinear coupled output complex networks subject to innovation constraints. *IEEE/CAA J. Autom. Sin.*, **2022**, *9*, 941–944. doi: [10.1109/JAS.2022.105581](https://doi.org/10.1109/JAS.2022.105581)
5. Ding, D.R.; Han, Q.L.; Ge, X.H.; *et al.* Secure state estimation and control of cyber-physical systems: A survey. *IEEE Trans. Syst. Man Cybern. Syst.*, **2021**, *51*, 176–190. doi: [10.1109/TSMC.2020.3041121](https://doi.org/10.1109/TSMC.2020.3041121)
6. Ciunzo, D.; Aubry, A.; Carotenuto, V. Rician MIMO channel- and jamming-aware decision fusion. *IEEE Trans. Signal Process.*, **2017**, *65*, 3866–3880. doi: [10.1109/TSP.2017.2686375](https://doi.org/10.1109/TSP.2017.2686375)
7. Leong, A.S.; Dey, S.; Nair, G.N. Quantized filtering schemes for multi-sensor linear state estimation: Stability and performance under high rate quantization. *IEEE Trans. Signal Process.*, **2013**, *61*, 3852–3865. doi: [10.1109/TSP.2013.2264465](https://doi.org/10.1109/TSP.2013.2264465)
8. Yu, M.; Wang, L.; Chu, T.G.; *et al.* Stabilization of networked control systems with data packet dropout and transmission delays: Continuous-time case. *Eur. J. Control.*, **2005**, *11*, 40–49. doi: [10.3166/ejc.11.40-49](https://doi.org/10.3166/ejc.11.40-49)
9. Li, Y.J.; Liu, G.P.; Sun, S.L.; *et al.* Prediction-based approach to finite-time stabilization of networked control systems with time delays and data packet dropouts. *Neurocomputing*, **2019**, *329*, 320–328. doi: [10.1016/j.neucom.2018.09.057](https://doi.org/10.1016/j.neucom.2018.09.057)
10. Bu, X.Y.; Dong, H.L.; Han, F.; *et al.* Event-triggered distributed filtering over sensor networks with deception attacks and partial measurements. *Int. J. Gen. Syst.*, **2018**, *47*, 522–534. doi: [10.1080/03081079.2018.1462353](https://doi.org/10.1080/03081079.2018.1462353)
11. Cui, P.; Zhang, H.S.; Lam, J.; *et al.* Real-time Kalman filtering based on distributed measurements. *Int. J. Robust Nonlinear Control*, **2013**, *23*, 1597–1608. doi: [10.1002/rnc.2848](https://doi.org/10.1002/rnc.2848)
12. Sinopoli, B.; Schenato, L.; Franceschetti, M.; *et al.* Kalman filtering with intermittent observations. *IEEE Trans. Autom. Control*, **2004**, *49*, 1453–1464. doi: [10.1109/TAC.2004.834121](https://doi.org/10.1109/TAC.2004.834121)
13. Wang, W.; Ma, L.F.; Rui, Q.Q.; *et al.* A survey on privacy-preserving control and filtering of networked control systems. *Int. J. Syst. Sci.*, **2024**, *55*, 2269–2288. doi: [10.1080/00207721.2024.2343734](https://doi.org/10.1080/00207721.2024.2343734)
14. Gao, P.X.; Jia, C.Q.; Zhou, A.Z. Encryption–decryption-based state estimation for nonlinear complex networks subject to coupled perturbation. *Syst. Sci. Control Eng.*, **2024**, *12*, 2357796. doi: [10.1080/21642583.2024.2357796](https://doi.org/10.1080/21642583.2024.2357796)
15. Yuan, M.M.; Qian, W. Adaptive output feedback tracking control for nonlinear systems with unknown growth rate. *Int. J. Netw. Dyn. Intell.*, **2024**, *3*, 100002. doi: [10.53941/ijndi.2024.100002](https://doi.org/10.53941/ijndi.2024.100002)
16. Wang, W.; Wang, M. Adaptive neural event-triggered output-feedback optimal tracking control for discrete-time pure-feedback nonlinear systems. *Int. J. Netw. Dyn. Intell.*, **2024**, *3*, 100010. doi: [10.53941/ijndi.2024.100010](https://doi.org/10.53941/ijndi.2024.100010)
17. Boutayeb, M.; Aubry, D. A strong tracking extended Kalman observer for nonlinear discrete-time systems. *IEEE Trans. Autom. Control*, **1999**, *44*, 1550–1556. doi: [10.1109/9.780419](https://doi.org/10.1109/9.780419)
18. Kai, X.; Wei, C.L.; Liu, L.D. Robust extended Kalman filtering for nonlinear systems with stochastic uncertainties. *IEEE Trans. Syst. Man Cybern. Part A Syst. Hum.*, **2010**, *40*, 399–405. doi: [10.1109/TSMCA.2009.2034836](https://doi.org/10.1109/TSMCA.2009.2034836)
19. Zhang, Y.J.; Li, M.; Zhang, Y.; *et al.* An enhanced adaptive unscented Kalman filter for vehicle state estimation. *IEEE Trans. Instrum. Meas.*, **2022**, *71*, 6502412. doi: [10.1109/TIM.2022.3180407](https://doi.org/10.1109/TIM.2022.3180407)
20. Li, L.; Yu, D.D.; Xia, Y.Q.; *et al.* Stochastic stability of a modified unscented Kalman filter with stochastic nonlinearities and multiple fading measurements. *J. Franklin Inst.*, **2017**, *354*, 650–667. doi: [10.1016/j.jfranklin.2016.10.028](https://doi.org/10.1016/j.jfranklin.2016.10.028)
21. Julier, S.J.; Uhlmann, J.K. Unscented filtering and nonlinear estimation. *Proc. IEEE*, **2004**, *92*, 401–422. doi: [10.1109/JPROC.2003.823141](https://doi.org/10.1109/JPROC.2003.823141)
22. Julier, S.; Uhlmann, J.; Durrant-Whyte, H.F. A new method for the nonlinear transformation of means and covariances in filters and estimators. *IEEE Trans. Autom. Control*, **2000**, *45*, 477–482. doi: [10.1109/9.847726](https://doi.org/10.1109/9.847726)
23. Hernandez-Gonzalez, M.; Basin, M.; Stepanov, O. Discrete-time state estimation for stochastic polynomial systems over polynomial observations. *Int. J. Gen. Syst.*, **2018**, *47*, 460–476. doi: [10.1080/03081079.2018.1461098](https://doi.org/10.1080/03081079.2018.1461098)
24. Liu, T.J.; Wang, Z.D.; Liu, Y.; *et al.* Unscented-Kalman-filter-based remote state estimation for complex networks with quantized measurements and amplify-and-forward relays. *IEEE Trans. Cybern.*, **2024**, *54*, 6819–6831. doi: [10.1109/TCYB.2024.3446649](https://doi.org/10.1109/TCYB.2024.3446649)
25. Li, C.Y.; Wang, Z.D.; Song, W.H.; *et al.* Resilient unscented Kalman filtering fusion with dynamic event-triggered scheme: Applications to multiple unmanned aerial vehicles. *IEEE Trans. Control Syst. Technol.*, **2023**, *31*, 370–381. doi: [10.1109/TCST.2022.3180942](https://doi.org/10.1109/TCST.2022.3180942)
26. Hu, J.; Wang, Z.D.; Alsaadi, F.E.; *et al.* Event-based filtering for time-varying nonlinear systems subject to multiple missing measurements with uncertain missing probabilities. *Inf. Fusion*, **2017**, *38*, 74–83. doi: [10.1016/j.inffus.2017.03.003](https://doi.org/10.1016/j.inffus.2017.03.003)
27. Dai, D.Y.; Li, J.H.; Song, Y.H.; *et al.* Event-based recursive filtering for nonlinear bias-corrupted systems with amplify-and-forward relays. *Syst. Sci. Control Eng.*, **2024**, *12*, 2332419. doi: [10.1080/21642583.2024.2332419](https://doi.org/10.1080/21642583.2024.2332419)
28. Wang, W.; Nešić, D.; Postoyan, R. Emulation-based stabilization of networked control systems implemented on FlexRay. *Automatica*, **2015**, *59*, 73–83. doi: [10.1016/j.automatica.2015.06.010](https://doi.org/10.1016/j.automatica.2015.06.010)
29. Cui, G.F.; Wu, L.B.; Wu, M. Adaptive event-triggered fault-tolerant control for leader-following consensus of multi-agent systems. *Int. J. Syst. Sci.*, **2024**, *55*, 3291–3303. doi: [10.1080/00207721.2024.2367074](https://doi.org/10.1080/00207721.2024.2367074)
30. Zhang, R.; Liu, H.J.; Liu, Y.F.; *et al.* Dynamic event-triggered state estimation for discrete-time delayed switched neural networks

- with constrained bit rate. *Syst. Sci. Control Eng.*, **2024**, *12*: 2334304. doi: [10.1080/21642583.2024.2334304](https://doi.org/10.1080/21642583.2024.2334304)
31. Wu, Y.B.; Niu, Y.G.; Yang, Y.K. Security sliding mode control for T-S fuzzy systems under attack probability-dependent dynamic round-robin protocol. *Int. J. Syst. Sci.*, **2024**, *55*: 926–940. doi: [10.1080/00207721.2023.2301037](https://doi.org/10.1080/00207721.2023.2301037)
  32. Cao, Z.R.; Niu, Y.G.; Karimi, H.R. Sliding mode control of automotive electronic valve system under weighted try-once-discard protocol. *Inf. Sci.*, **2020**, *515*: 324–340. doi: [10.1016/j.ins.2019.12.032](https://doi.org/10.1016/j.ins.2019.12.032)
  33. Li, C.Y.; Liu, Y.F.; Gao, M.; *et al.* Fault-tolerant formation consensus control for time-varying multi-agent systems with stochastic communication protocol. *Int. J. Netw. Dyn. Intell.*, **2024**, *3*: 100004. doi: [10.53941/ijndi.2024.100004](https://doi.org/10.53941/ijndi.2024.100004)
  34. Liu, S.; Wang, Z.D.; Wang, L.C.; *et al.* Recursive set-membership state estimation over a FlexRay network. *IEEE Trans. Syst. Man Cybern. Syst.*, **2022**, *52*: 3591–3601. doi: [10.1109/TSMC.2021.3071390](https://doi.org/10.1109/TSMC.2021.3071390)
  35. Wang, W.; Nešić, D.; Postoyan, R. Observer design for networked control systems with FlexRay. *Automatica*, **2017**, *82*: 42–48. doi: [10.1016/j.automatica.2017.03.038](https://doi.org/10.1016/j.automatica.2017.03.038)
  36. Makowitz, R.; Temple, C. Flexray-a communication network for automotive control systems. In *Proceedings of 2006 IEEE International Workshop on Factory Communication Systems, Turin, Italy, 28–30 June 2006*; IEEE: New York, 2006; pp. 207–212. doi: [10.1109/WFCS.2006.1704153](https://doi.org/10.1109/WFCS.2006.1704153)
  37. Shaw, R.; Jackman, B. An introduction to FlexRay as an industrial network. In *Proceedings of 2008 IEEE International Symposium on Industrial Electronics, Cambridge, UK, 30 June 2008–02 July 2008*; IEEE: New York, 2008; pp. 1849–1854. doi: [10.1109/ISIE.2008.4676987](https://doi.org/10.1109/ISIE.2008.4676987)
  38. Liu, S.; Wang, Z.D.; Wang, L.C.; *et al.* Finite-horizon  $H_\infty$  filtering via a high-rate network with the FlexRay protocol. *IEEE Trans. Autom. Control*, **2023**, *68*: 3596–3603. doi: [10.1109/TAC.2022.3190791](https://doi.org/10.1109/TAC.2022.3190791)
  39. Zheng, C.C.; Fu, H.; Bai, J.J.; *et al.* FlexRay protocol based distributed nonfragile dissipative filtering of state-saturated switched stochastic systems. *Int. J. Syst. Sci.*, **2024**, *55*: 714–727. doi: [10.1080/00207721.2023.2293685](https://doi.org/10.1080/00207721.2023.2293685)
  40. Li, X.; Cheng, K.J.; Wang, Z.H.; *et al.* Distributed interval observer-based robust control for multirate systems under the FlexRay protocol. *J. Franklin Inst.*, **2024**, *361*: 106708. doi: [10.1016/j.jfranklin.2024.106708](https://doi.org/10.1016/j.jfranklin.2024.106708)
  41. Hu, J.; Wang, Z.D.; Chen, D.Y.; *et al.* Estimation, filtering and fusion for networked systems with network-induced phenomena: New progress and prospects. *Inf. Fusion*, **2016**, *31*: 65–75. doi: [10.1016/j.inffus.2016.01.001](https://doi.org/10.1016/j.inffus.2016.01.001)
  42. Li, W.L.; Sun, S.H.; Jia, Y.M.; *et al.* Robust unscented Kalman filter with adaptation of process and measurement noise covariances. *Digit. Signal Process.*, **2016**, *48*: 93–103. doi: [10.1016/j.dsp.2015.09.004](https://doi.org/10.1016/j.dsp.2015.09.004)
  43. Wang, Y.Z.; Wang, Z.D.; Zou, L.; *et al.* Ultimately bounded PID control for T-S fuzzy systems under FlexRay communication protocol. *IEEE Trans. Fuzzy Syst.*, **2023**, *31*: 4308–4320. doi: [10.1109/TFUZZ.2023.3282044](https://doi.org/10.1109/TFUZZ.2023.3282044)
  44. Liu, S.; Wang, Z.D.; Chen, Y.; *et al.* Protocol-based unscented Kalman filtering in the presence of stochastic uncertainties. *IEEE Trans. Autom. Control*, **2020**, *65*: 1303–1309. doi: [10.1109/TAC.2019.2929817](https://doi.org/10.1109/TAC.2019.2929817)
  45. Geng, H.; Mousavi, A.; Markatos, N.G.; *et al.* Reliable cost prediction and control for intelligent manufacture: a key performance indicator perspective. *Int. J. Netw. Dyn. Intell.*, **2024**, *3*: 100001. doi: [10.53941/ijndi.2024.100001](https://doi.org/10.53941/ijndi.2024.100001)
  46. Geng, H.; Wang, Z.D.; Ma, L.F.; *et al.* Distributed filter design over sensor networks under try-once-discard protocol: Dealing with sensor-bias-corrupted measurement censoring. *IEEE Trans. Syst. Man Cybern. Syst.*, **2024**, *54*: 3032–3043. doi: [10.1109/TSMC.2024.3354883](https://doi.org/10.1109/TSMC.2024.3354883)

**Citation:** Meng, X.; Wang, H.; Li, Y.; *et al.* Unscented Kalman Filtering for Nonlinear Systems with Stochastic Nonlinearities under FlexRay Protocol. *International Journal of Network Dynamics and Intelligence*. 2025, 4(2), 100010. doi: [10.53941/ijndi.2025.100010](https://doi.org/10.53941/ijndi.2025.100010)

**Publisher’s Note:** Scilight stays neutral with regard to jurisdictional claims in published maps and institutional affiliations.